NASA/CR–2014-218666

# Elemental Water Impact Test: Phase 3 Plunge Depth of a 36-inch Aluminum Tank Head

*Gregory J. Vassilakos*
*Analytical Mechanics Associates, Inc., Hampton, Virginia*

December 2014

## NASA STI Program . . . in Profile

Since its founding, NASA has been dedicated to the advancement of aeronautics and space science. The NASA scientific and technical information (STI) program plays a key part in helping NASA maintain this important role.

The NASA STI program operates under the auspices of the Agency Chief Information Officer. It collects, organizes, provides for archiving, and disseminates NASA's STI. The NASA STI program provides access to the NTRS Registered and its public interface, the NASA Technical Reports Server, thus providing one of the largest collections of aeronautical and space science STI in the world. Results are published in both non-NASA channels and by NASA in the NASA STI Report Series, which includes the following report types:

- TECHNICAL PUBLICATION. Reports of completed research or a major significant phase of research that present the results of NASA Programs and include extensive data or theoretical analysis. Includes compilations of significant scientific and technical data and information deemed to be of continuing reference value. NASA counter-part of peer-reviewed formal professional papers but has less stringent limitations on manuscript length and extent of graphic presentations.

- TECHNICAL MEMORANDUM. Scientific and technical findings that are preliminary or of specialized interest, e.g., quick release reports, working papers, and bibliographies that contain minimal annotation. Does not contain extensive analysis.

- CONTRACTOR REPORT. Scientific and technical findings by NASA-sponsored contractors and grantees.

- CONFERENCE PUBLICATION. Collected papers from scientific and technical conferences, symposia, seminars, or other meetings sponsored or co-sponsored by NASA.

- SPECIAL PUBLICATION. Scientific, technical, or historical information from NASA programs, projects, and missions, often concerned with subjects having substantial public interest.

- TECHNICAL TRANSLATION. English-language translations of foreign scientific and technical material pertinent to NASA's mission.

Specialized services also include organizing and publishing research results, distributing specialized research announcements and feeds, providing information desk and personal search support, and enabling data exchange services.

For more information about the NASA STI program, see the following:

- Access the NASA STI program home page at http://www.sti.nasa.gov

- E-mail your question to help@sti.nasa.gov

- Phone the NASA STI Information Desk at 757-864-9658

- Write to:
  NASA STI Information Desk
  Mail Stop 148
  NASA Langley Research Center
  Hampton, VA 23681-2199

NASA/CR–2014-218666

# Elemental Water Impact Test: Phase 3 Plunge Depth of a 36-inch Aluminum Tank Head

*Gregory J. Vassilakos*
*Analytical Mechanics Associates, Inc., Hampton, Virginia*

National Aeronautics and
Space Administration

Langley Research Center
Hampton, Virginia 23681-2199

Prepared for Langley Research Center
under Contract NNL12AA09C

December 2014

## Acknowledgments

The author would like to recognize Dr. Karen Lyle for her role in conceiving the EWIT test plan, and Steve Gayle for spearheading the set-up of the test pool and procurement of the test articles. The author would also like to recognize David Stegall for conducting the tests and overseeing the data acquisition system operations performed by Amanda Pettit-Pokora and Brian Shank, and Dr. Justin Littell for setting up and operating the photogrammetry system.



Available from:

NASA STI Program / Mail Stop 148
NASA Langley Research Center
Hampton, VA 23681-2199
Fax: 757-864-6500

# Abstract

*Spacecraft are being designed based on LS-DYNA water landing simulations. The Elemental Water Impact Test (EWIT) series was undertaken to assess the accuracy of LS-DYNA water impact simulations. Phase 3 featured a composite tank head that was tested at a range of heights to verify the ability to predict structural failure of composites. To support planning for Phase 3, a test series was conducted with an aluminum tank head dropped from heights of 2, 6, 10, and 12 feet to verify that the test article would not impact the bottom of the test pool. This report focuses on the comparisons of the measured plunge depths to LS-DYNA predictions. The results for the tank head model demonstrated the following.*

1. *LS-DYNA provides accurate predictions for peak accelerations.*
2. *LS-DYNA consistently under-predicts plunge depth. An allowance of at least 20% should be added to the LS-DYNA predictions.*
3. *The LS-DYNA predictions for plunge depth are relatively insensitive to the fluid-structure coupling stiffness.*

# Table of Contents

# List of Figures



# List of Tables

# 1. Introduction

Spacecraft are being designed based on LS-DYNA [1] water landing simulations. The Elemental Water Impact Test (EWIT) series was undertaken to assess the accuracy of LS-DYNA water impact simulations. Phase 1 of the EWIT test series featured water drop tests of a 20-inch spherical penetrometer, and focused on acceleration and pressure measurements [2]. Phase 2 featured a 36-inch aluminum tank head machined down to a minimal thickness and outfitted with accelerometers, pressure transducers, deflection gages, and strain gages [3]. Phase 3 featured a composite tank head that was tested at a range of heights to verify the ability to predict structural failure of composites. To support planning for Phase 3, a test series was conducted with an aluminum tank head dropped from heights of 2, 6, 10, and 12 feet to verify that the test article would not impact the bottom of the test pool. This report focuses on the comparisons of the measured plunge depths to LS-DYNA predictions.

# 2. Tests

## 2.1. Test Configuration

The drop tests were performed in a 15-foot above-ground swimming pool. The test pool was located inside a 24-foot above-ground swimming pool to catch any over splash. A foam pad existed under the floor of the inner pool to cushion the blow from bottom impacts. The test article was suspended above the test pool via a forklift. A line hanging from the test article was used to measure the drop height. Water impact tests were performed at drop heights of 2, 6, 10, and 12 feet. The test set-up is illustrated in Figure 1.

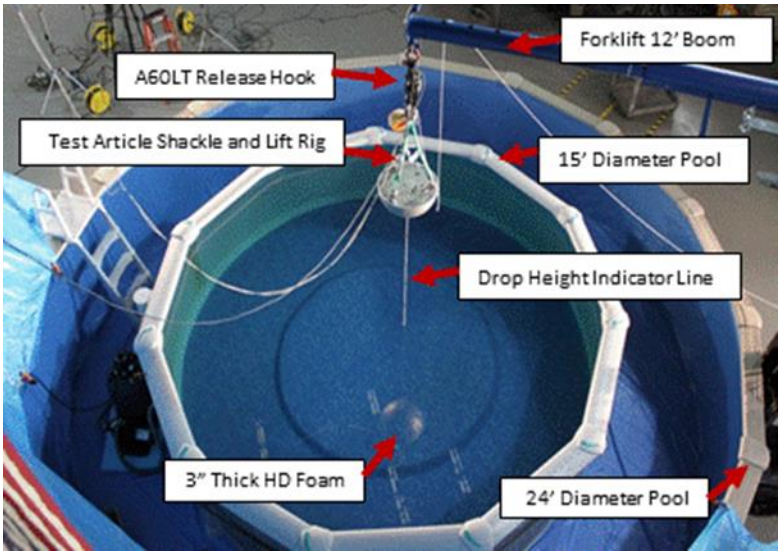


*Figure 1. Test Set-Up*

## 2.2. Test Article

The test article was an aluminum tank head with a nominal shell thickness of 0.188 inches. The diameter at the rim was approximately 36 inches, the radius of curvature at the center was approximately 34 inches, and the depth from the rim to the apex was approximately 7.7 inches. The tank head was outfitted with an aluminum cover with a thickness of 0.5 inches. The cover was attached to the tank head via an aluminum

bolting ring with an outer radius of 17.8 inches, an inner radius of 14.1 inches, and a thickness of 1.5 inches. The bolting ring connected to the tank head via twelve quarter-inch steel bolts and to the cover via twelve three-eighths-inch steel bolts. The tank head was outfitted with a three-axis accelerometer and two photogrammetry target towers. The total weight of the test article with instrumentation, lifting bridal, and photogrammetry towers was approximately 135 lbs. The test article is illustrated in Figure 2.

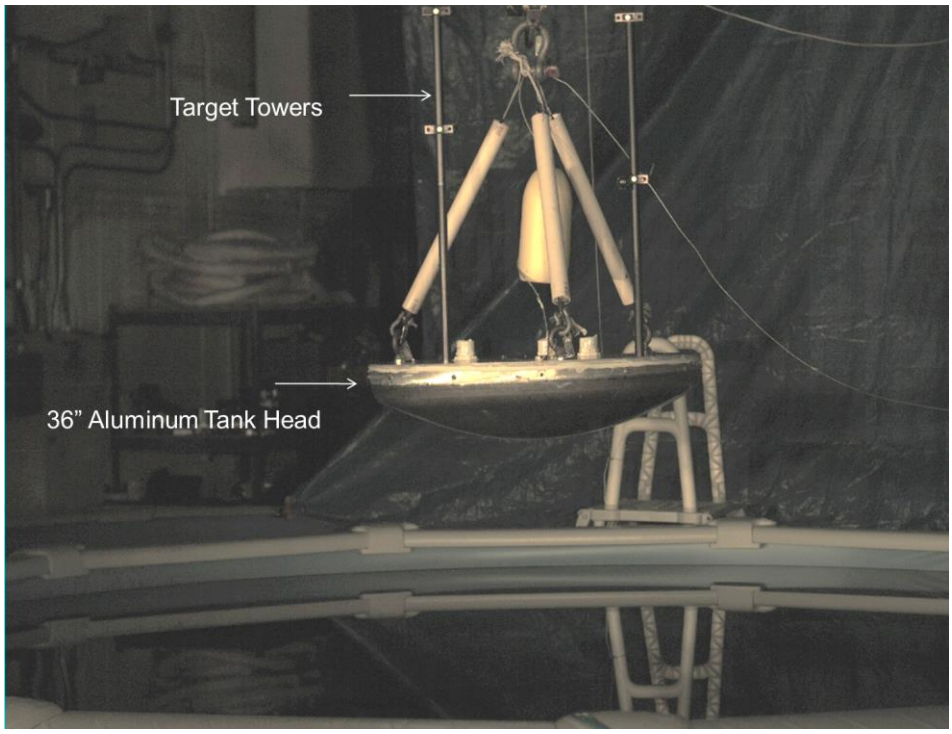


*Figure 2. Test Article*

## 3. Simulations

### 3.1. LS-DYNA

LS-DYNA is a general purpose transient dynamic finite element code capable of simulating complex real world problems. LS-DYNA's strength is in the modeling of impact problems. An explicit time integration scheme is used in which there is no equilibrium check and no iteration of the solution between time steps. This approach works only because the time step is restricted to be smaller than the shortest stress wave transit time for any element in the model.

A key strength of LS-DYNA is the modeling of contact between bodies. This is accomplished via a penalty method. Contact is detected when the nodes of one body pass through the face or edges of the elements of another body. Preloaded penalty springs are then inserted to push the bodies apart. One consequence of this approach is one body must always penetrate another body before contact is detected. Another consequence is that there is a finite contact stiffness at the interface between the bodies that is entirely nonphysical.

LS-DYNA has a limited capability to model a fluid using Arbitrary Lagrangian-Eulerian (ALE) meshes. In the ALE approach, each time step begins with a mesh that is conceptually similar to the Lagrangian

meshes used to model structures. LS-DYNA determines the deformation of the fluid that occurs during the time step, then moves, or advects, the mesh back to its original configuration and treats the fluid as having moved through the mesh. The result is that the nodes of the mesh do not move. Instead, the volume fraction of the fluid in each element is changed. The fluid in the ALE mesh can flow, compress, and impart momentum; however, the ALE mesh does not offer a full Navier-Stokes fluid flow solution.

### 3.2. LS-DYNA Model

An LS-DYNA model was created of the tank head and a portion of the water within the test pool. One quarter of the structure and water region was modeled and symmetry boundary conditions were applied. The model featured shell elements for the tank head and the cover plate. The nominal element size was 0.4 inches. The tank head material was treated as rigid. A uniform thickness of 0.1 inches was assigned to the structure and the mass density was adjusted to give a weight corresponding to 133.5 lbs. for the full structure, which approximately corresponds to the weight of the outfitted test article without the lifting bridle.

A cylindrical water mesh was provided with a radius of 60 inches, a water depth of 48 inches, and an air height of 36 inches. The nominal element size at the center of the mesh was 1 inch. Equations of state were specified for the both the air and water. Reservoir elements were specified at the outer radius and top, which allowed fluid to flow in and out of the mesh while maintaining constant pressure at the boundary. The model is illustrated in Figure 3.

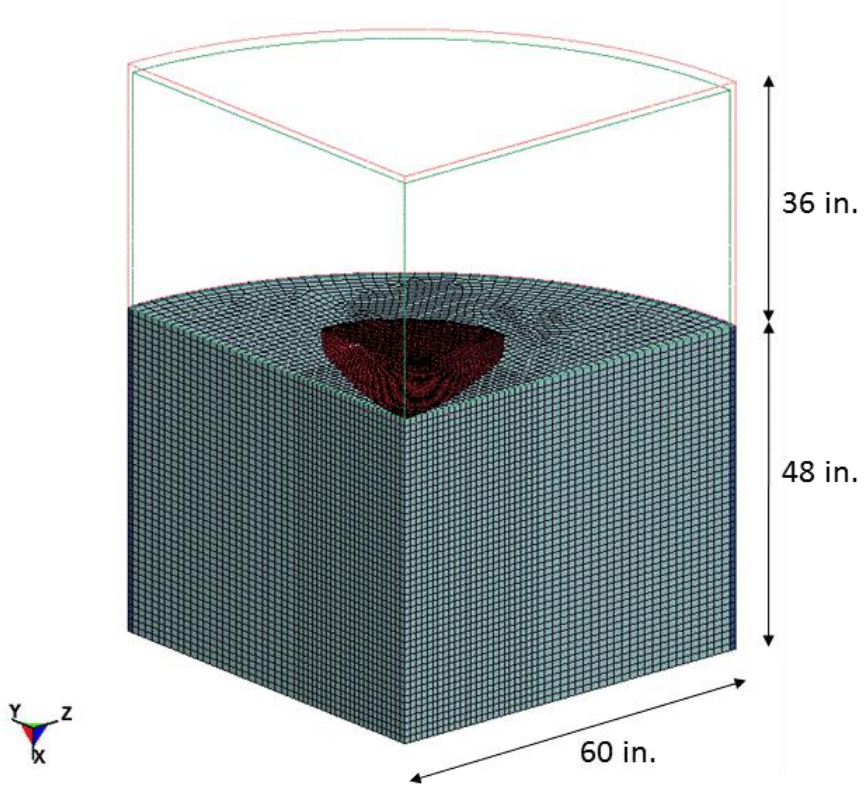


*Figure 3. LS-DYNA Model*

The air and water were initialized with atmospheric pressure (14.7 psi) at the water surface plus hydrostatic pressure due to gravity below the water surface. The equations of state for the water and air were specified as linear polynomials with the parameters shown in Table 1.

*Table 1. Air and Water Equation of State Parameters*

| Water | |
|---|---|
| Mass Density, $\rho$ | 9.3365E-5 lb-sec$^2$/in |
| Free Surface Pressure, $p_0$ | 14.7 psi |
| Bulk Modulus, K | 3.11574E5 psi |
| Air | |
| Mass Density, $\rho$ | 1.127E-7 lb-sec$^2$/in |
| Specific Heat Capacity Ratio, $\gamma = c_P/c_V$ | 1.4 |
| Internal Energy, $E_0$ | 36.74 psi |

Coupling was specified between the structure and the water only. The air interacted with the water, but not the structure. The coupling stiffness between the structure and the water was defined as a nonlinear curve referred to as "Curve 8" within this project. LS-DYNA utilizes a penalty method for coupling the structure to the fluid. The coupling stiffness curve specifies the pressure acting on the structure as a function of the penetration of the fluid into the structure. When penetration of fluid into the structure is detected, a spring is inserted. For penetration distances beyond the end of the curve, LS-DYNA linearly extrapolates the pressure based on the last two points of the curve. The "Curve 8" coupling stiffness curve is illustrated in Figure 4.

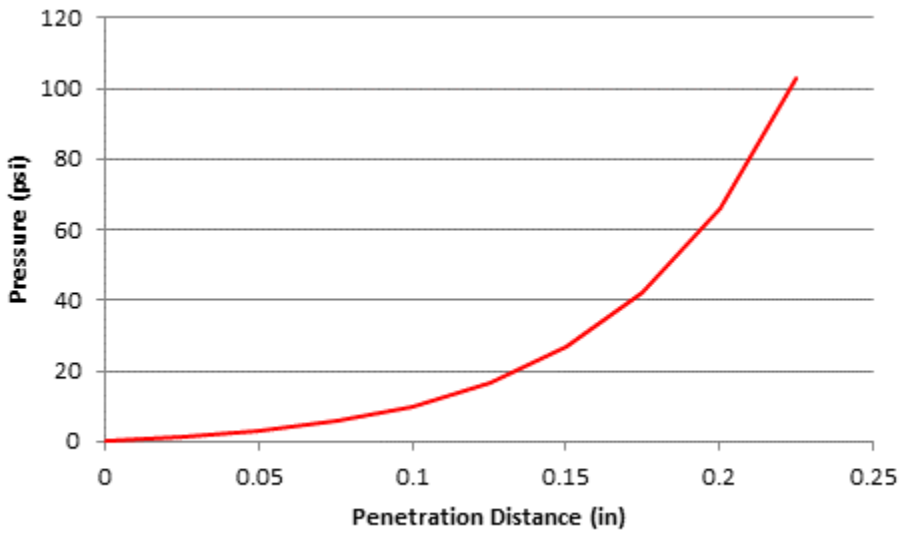


*Figure 4. Fluid-Structure Coupling Stiffness "Curve 8"*

The algorithm in LS-DYNA requires that there be some penetration of the fluid into the structure in order for there to be a coupling force. The term "penetration" should be understood as distinct from "leakage".

Penetration implies that a coupling force is pushing the fluid and structure apart. Leakage implies that a portion of the fluid has escaped through the structural boundary.

# 4. Data Processing

## 4.1. Plunge Depth Photogrammetry Measurements

Photogrammetry data for the positions of targets on towers mounted to the cover plate was recorded at 100 frames per second. The photogrammetry towers stood 36 inches above the top of the cover plate and did not fully submerge during the initial plunge. On return to the surface, the test article typically pitched to one side. The photogrammetry history for the 12-foot drop is illustrated in Figure 5. The data exhibits wobble, which is a reflection of the uncertainty in the location of the center of the target as determined by the software used to process the photogrammetry images. The wobble is estimated to be approximately 0.5 inches.

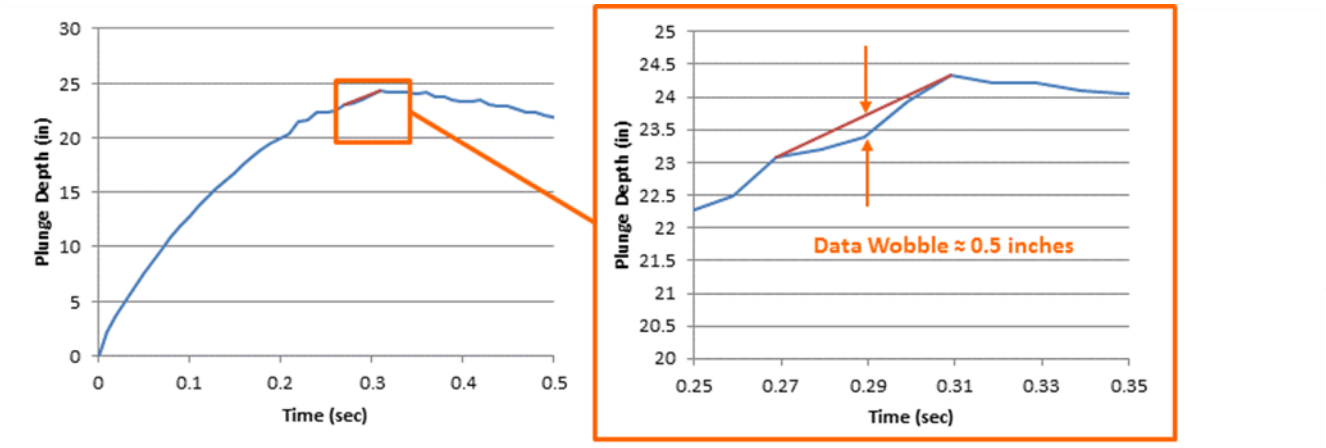


*Figure 5. Photogrammetry Plunge Depth Measurement for 12-foot Drop*

## 4.2. Acceleromter Data

Accelerometer data was recorded at a rate of 40,000 samples per second. The DAS featured an in-line 4300 Hz analog anti-aliasing filter. The data output from the DAS is referred to as the raw accelerometer data. For comparison with acceleration data from simulations, the raw accelerometer data was filtered with a 1000 Hz forward-backward Butterworth filter. The purpose of the filter was to ensure that test versus simulation comparisons were between acceleration histories with similar frequency content. Figure 6 shows raw and filtered accelerometer histories during the initial impact for the 12-foot drop. The filter frequency was high enough that the structural ringing of the test article is apparent in the filtered acceleration history.

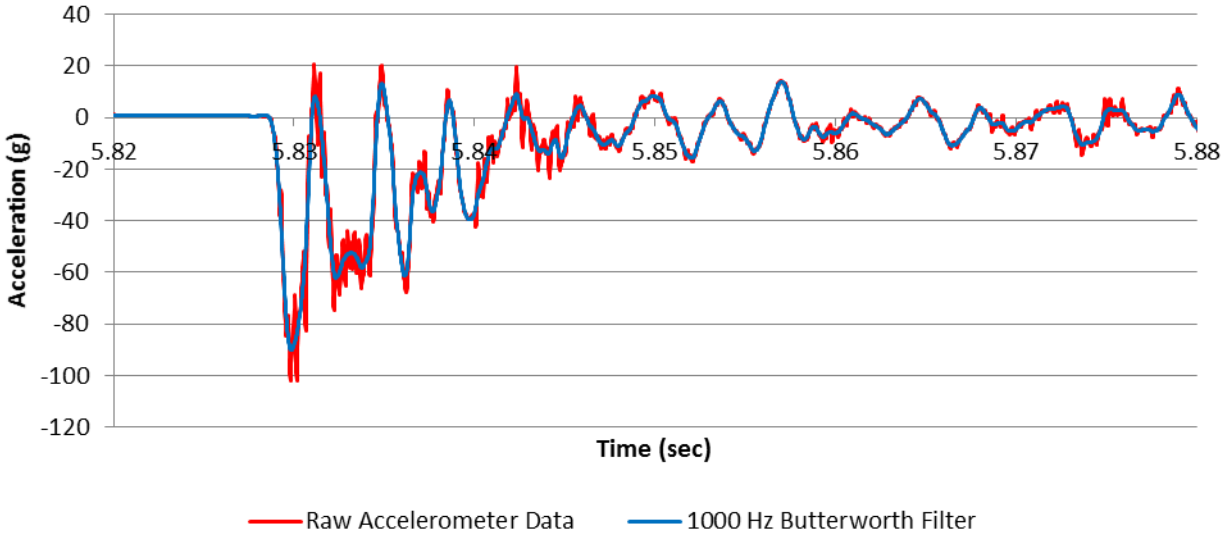


*Figure 6. Raw and Filtered Accelerometer Histories for 12-foot Drop*

### 4.3. Plunge Depth Calculation from Accelerometer Data

In order to determine the plunge depth, the raw accelerometer data was rezeroed to provide an average acceleration of 0 g prior to release. The rezeroed accelerometer data was then integrated to determine velocity. The velocity data was then rezeroed based on a short period prior to release and then was integrated to determine displacement. The time of release and time of impact were determined based on the sudden change in the acceleration. The plunge depth was then determined as the maximum displacement minus the displacement at the time of the spike in the acceleration. The acceleration, velocity, and displacement time histories for the 12-foot drop case are illustrated in Figure 7. Plunge depth time histories for all the tests from both photogrammetry and integrated accelerations are shown in Figure 8. Due to possible errors in the rezeroing that result in drift in the integrated response, the integrated accelerometer data is not considered any more accurate than the photogrammetry measurements. The two sets of measurements agree to within approximately one inch.

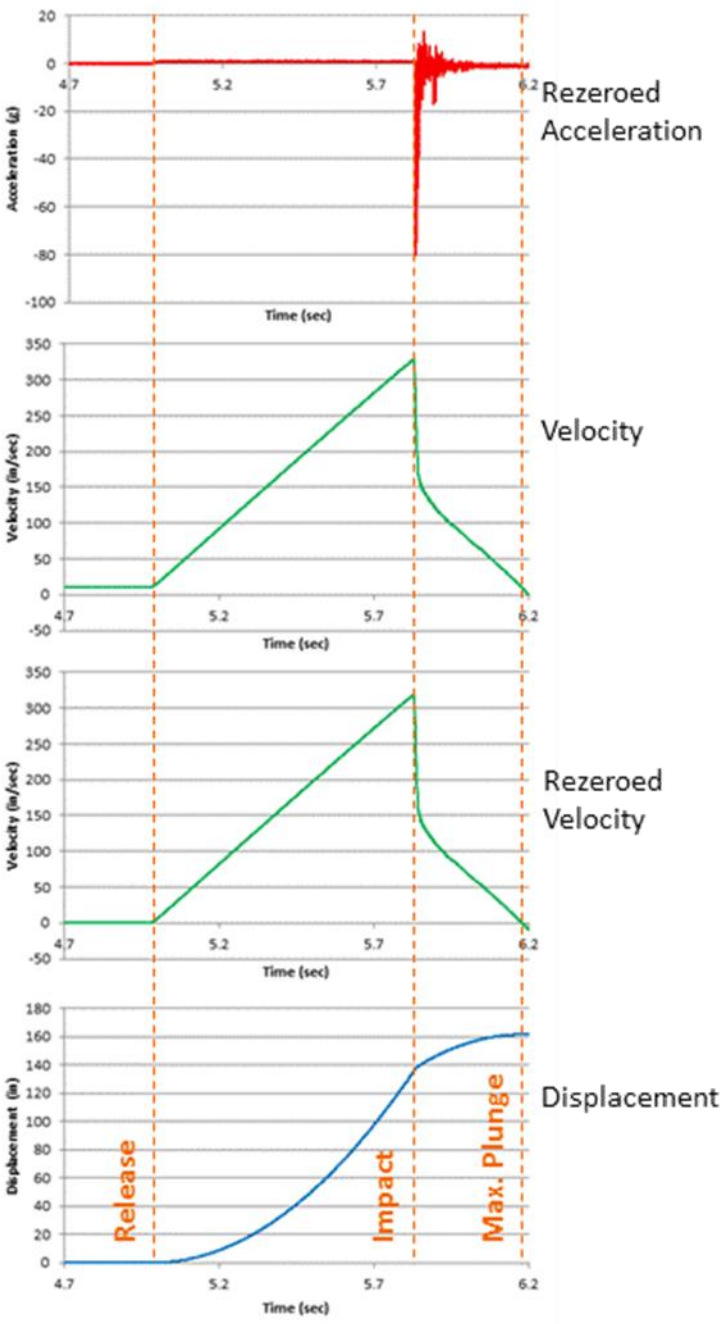


*Figure 7. Plunge Depth Integrated from Accelerometer Data for 12-foot Drop*

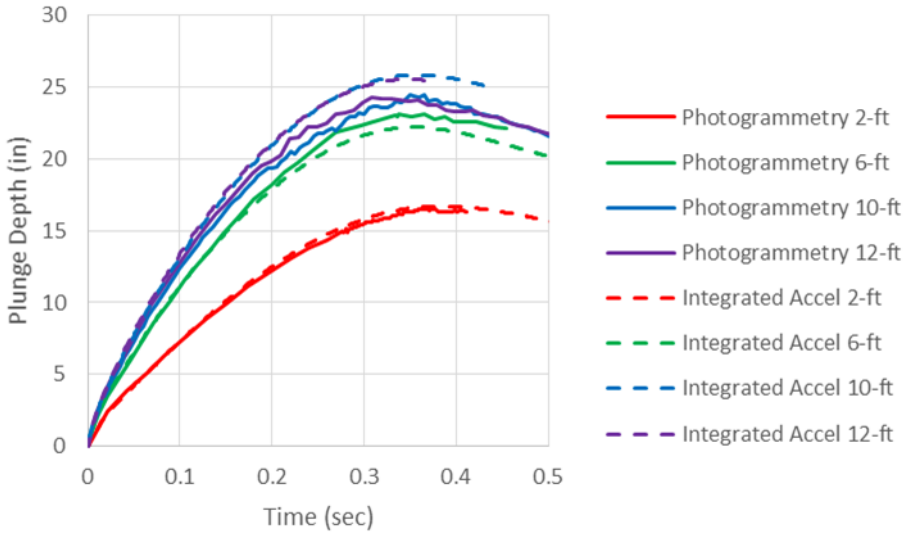


Figure 8. Test Plunge Depth Histories from Photogrammetry and Integrated Accelerations

### 4.4. Simulation Acceleration Data

The simulation acceleration data was processed through the same 1000 Hz forward-backward Butterworth filter used for the tests data. Since the simulation model was rigid, there was no structural ringing in the response, so the filter had little effect on the peak magnitudes. Filtered and unfiltered acceleration histories from simulations of the 12-foot drop are illustrated in Figure 9.

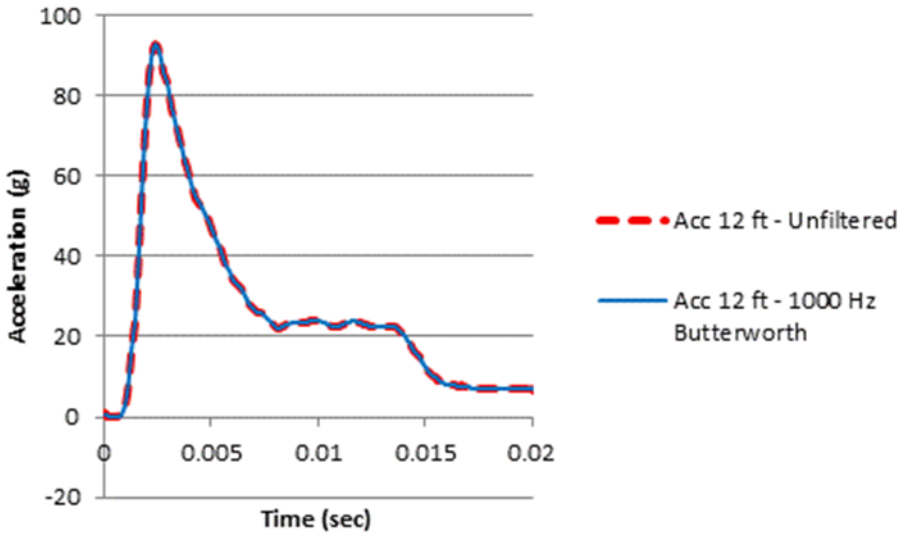


*Figure 9. Filtered and Unfiltered Simulation Acceleration Histories for 12-foot Drop*

## 5. Test and Simulation Results

### 5.1. Acceleration

Acceleration Histories from the tests and simulations are shown on Figure 10. The test acceleration histories have been adjusted to show -1g during free fall and positive acceleration during the impact. Arbitrary time shifts have been applied to approximately align the initial rise in the responses. Despite missing all the structural vibratory response, the peak accelerations from the rigid simulation model show an average absolute deviation from the test data of just 4%.

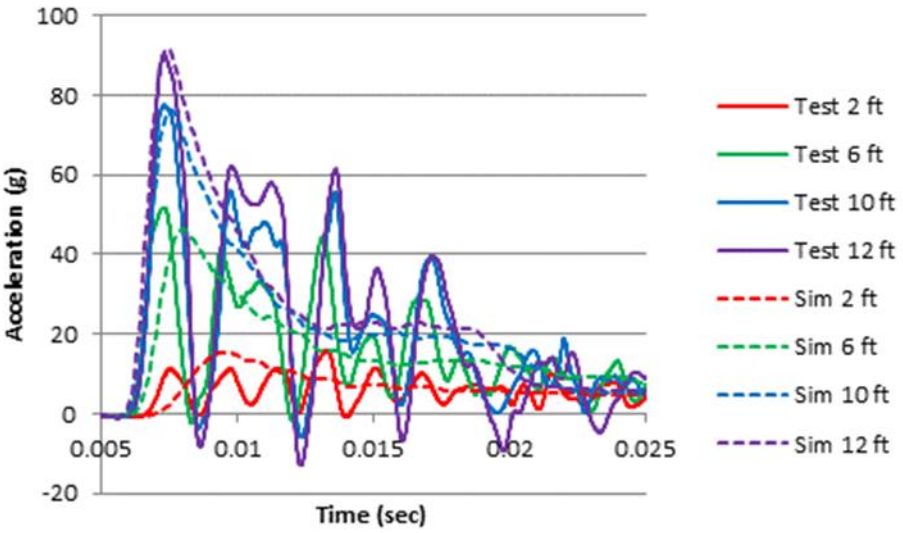


*Figure 10. Test and Simulation Acceleration Histories*

The peak accelerations from each test are listed in Table 2 and the simulation peaks are plotted against the test peaks in Figure 11. Both the test and simulation acceleration peaks are proportional to the square of the velocity as shown in Figure 12.

*Table 2. Peak Test and Simulation Accelerations*

| Drop Height (ft) | Impact Velocity (ft/sec) | Peak Test Acceleration (g) | Peak Simulation Acceleration (g) |
|---|---|---|---|
| 2 | 11.35 | 15.79 | 15.31 |
| 6 | 19.66 | 51.77 | 46.37 |
| 10 | 25.38 | 77.56 | 76.45 |
| 12 | 27.80 | 90.14 | 91.81 |

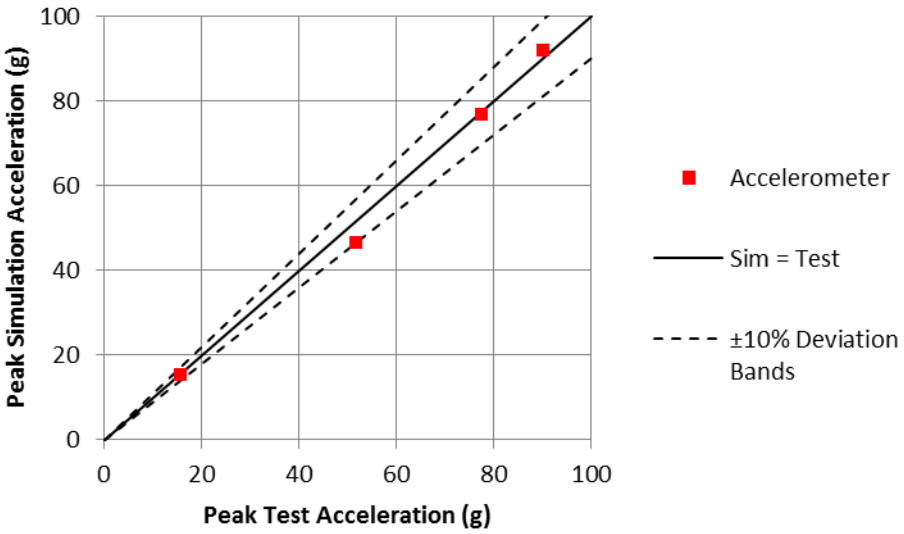


*Figure 11. Peak Test Acceleration vs. Peak Simulation Acceleration*

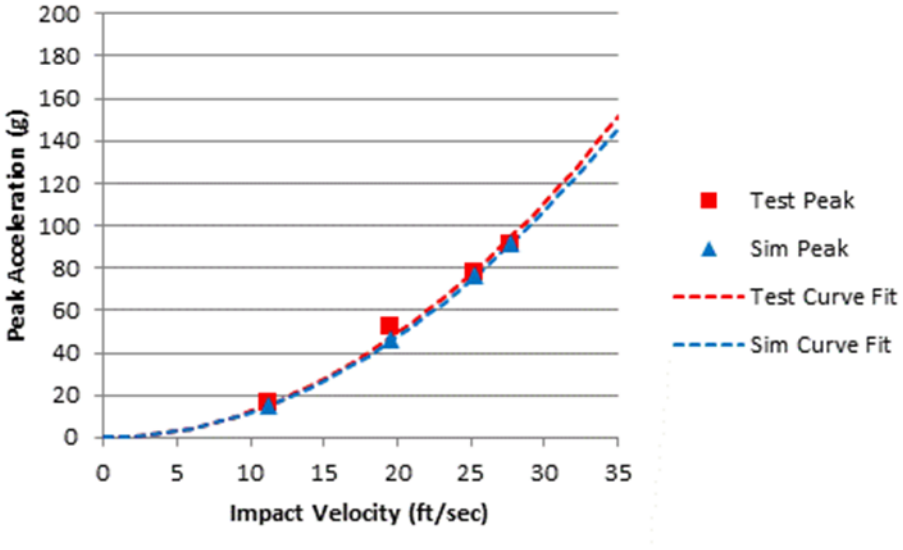


*Figure 12. Peak Test and Simulation Accelerations*

## 5.2. Plunge Depth

Figure 13 illustrates the test and simulation plunge depth histories. The test data is from photogrammetry. The plunge depths from the simulations and from both photogrammetry and the integrated accelerometer data are provided in Table 3 and the simulation plunge depths are plotted against the test plunge depths in Figure 14. Points to note are that the simulations consistently under-predict the plunge depth and that the plunge depth for the tests as a function of the drop height is highly nonlinear. The test for the 10-foot drop produced a plunge depth slightly deeper than the 12-foot drop. The test and simulation data track closely during the initial impact and then diverge, which is expected as the LS-DYNA water model is not

a Navier-Stokes fluid flow solver. Much of the physics of fluid flow is missing from the algorithm. Based on these findings, it is recommended that a margin of 20% be allowed when basing plunge depth predictions on LS-DYNA simulations.

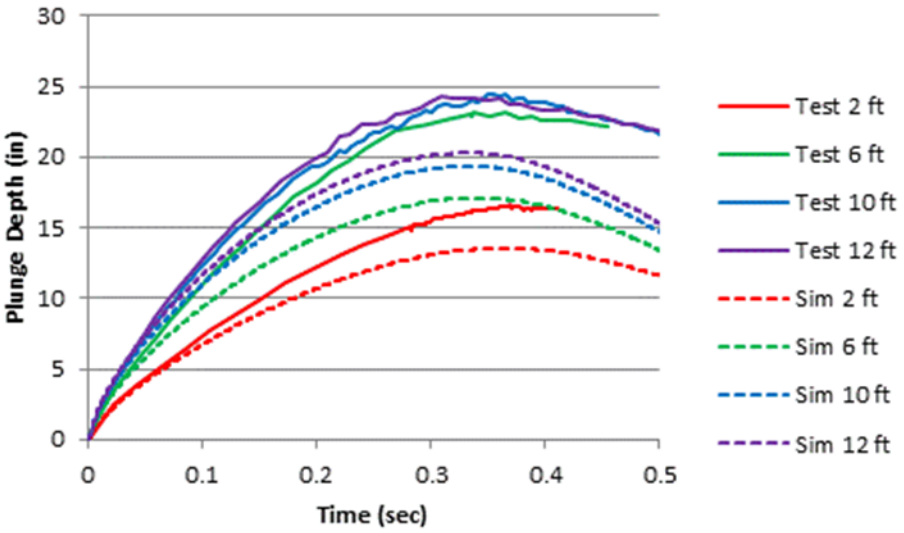


*Figure 13. Test and Simulation Plunge Depth Histories*

*Table 3. Test and Simulation Plunge Depths*

| Drop Height (ft) | Impact Velocity (ft/sec) | Test Plunge Depth Photogrammetry (in) | Test Plunge Depth Accelerometer (in) | Simulation Plunge Depth (in) |
|---|---|---|---|---|
| 2 | 11.35 | 16.59 | 16.71 | 13.53 |
| 6 | 19.66 | 23.13 | 22.22 | 17.11 |
| 10 | 25.38 | 24.46 | 25.86 | 19.36 |
| 12 | 27.80 | 24.34 | 25.56 | 20.29 |

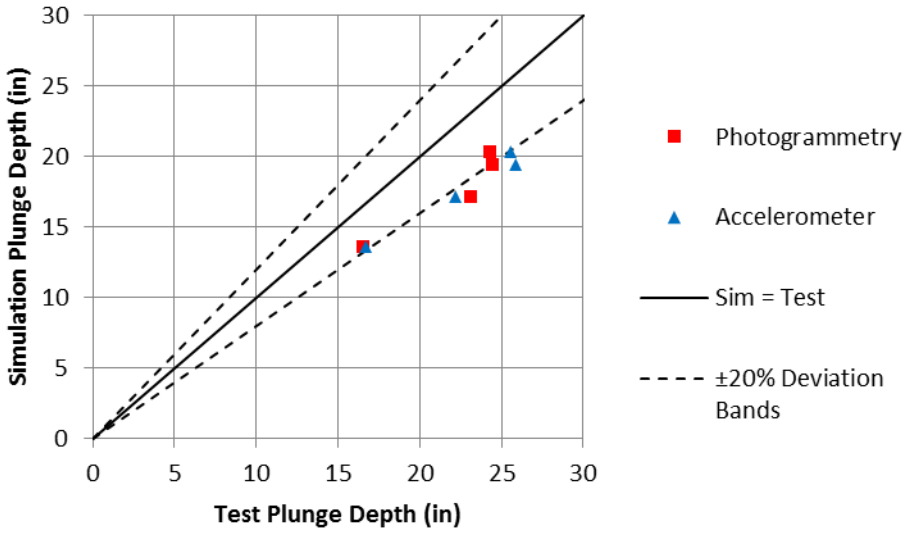


*Figure 14. Test Plunge Depth vs. Simulation Plunge Depth*

### 5.3. Motion Response

The gross motion seen in the test can be divided into four phases:

1. Initial Impact – The test article impacts the water surface upright.
2. Plunge – The test article plunges upright, opening a large cavitation volume above it.
3. Cavitation Closure – The cavitation volume closes and sends a plume to the surface.
4. Return to Surface – The test article capsizes as it gains velocity back toward the surface.

The four phases are illustrated in Figure 15. The images were extracted from underwater video of a six-foot drop test and are at one-third second intervals. The test article in the video was not the test article used for the plunge depth test series, but was similar in shape and weight.

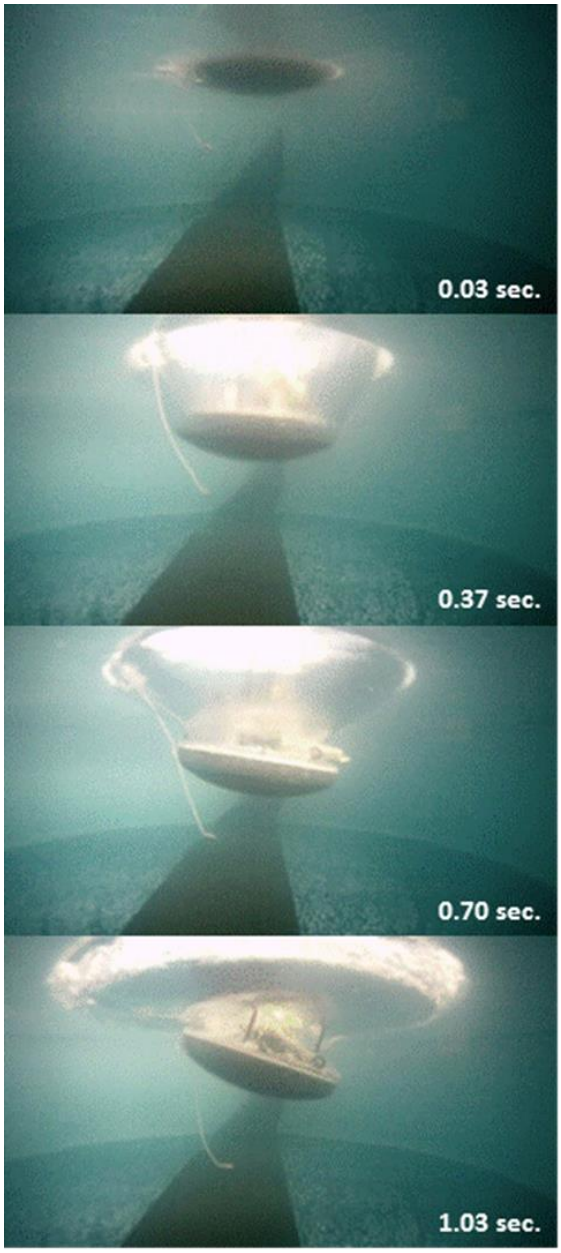


*Figure 15. Plunge Sequence for a 6-foot Drop Test*

Images from the simulations are provided in Figure 16. The simulations exhibit the same general response sequence observed in the tests. The major difference is that the model remains upright throughout the plunge and return to the surface. This is a consequence of the symmetry boundary conditions, which do not permit rotation.

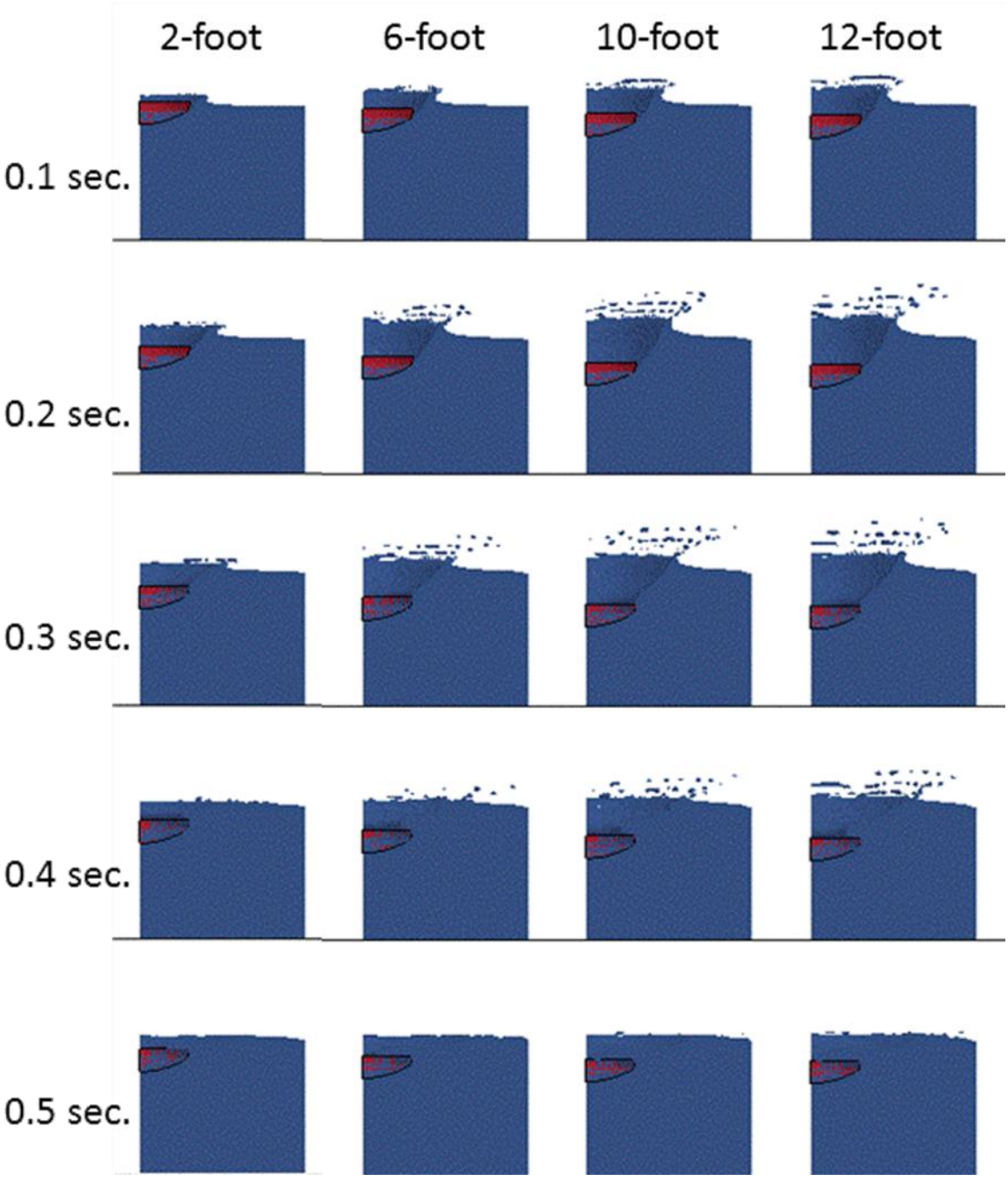


*Figure 16. Simulation Plunge Sequences*

## 6. Simulation Coupling Stiffness Sensitivity

The most important parameter in the LS-DYNA fluid-structure interaction algorithm is the coupling stiffness. Two coupling stiffness curves have been used for the simulations. These were the baseline curve referred to as Curve 8 and a stiffer variant referred to as Curve 11. Curve 8 and Curve 11 are

illustrated in Figure 17. It is believed that a finer water mesh requires a stiffer coupling stiffness curve, so the coupling stiffness curve should be considered mesh specific.

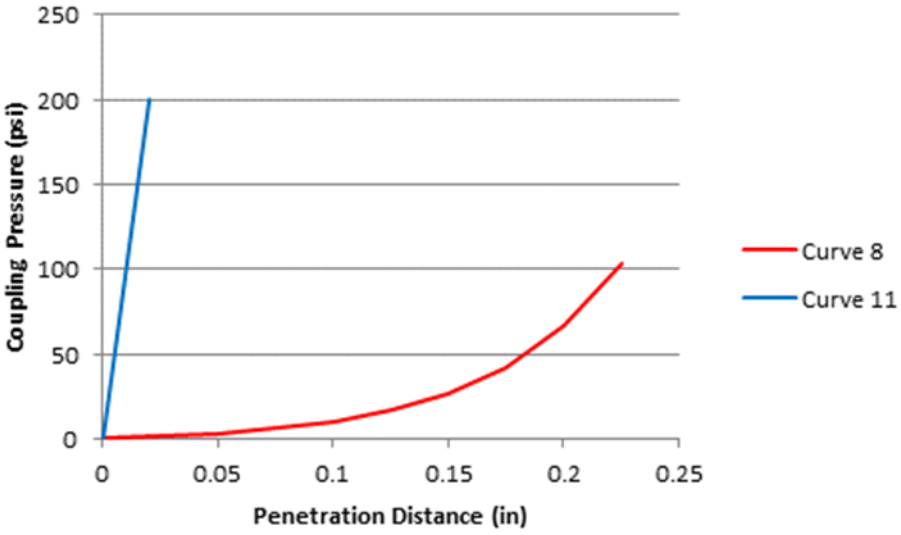


*Figure 17. Coupling Stiffness Curves*

Simulations with the two coupling stiffness curves were conducted with a drop height of 12 feet. The simulations showed the change in the plunge depth to be negligible as shown in Figure 18; however, there was significant difference in the acceleration as shown in Figure 19. The acceleration data was filtered with a forward-backward Butterworth filter with a cutoff frequency of 1000 Hz. The oscillation in the acceleration for the higher coupling stiffness case does not represent any real structural response as the structural model is rigid. The oscillation is an artifact of the compliance of the coupling stiffness and water compressibility.

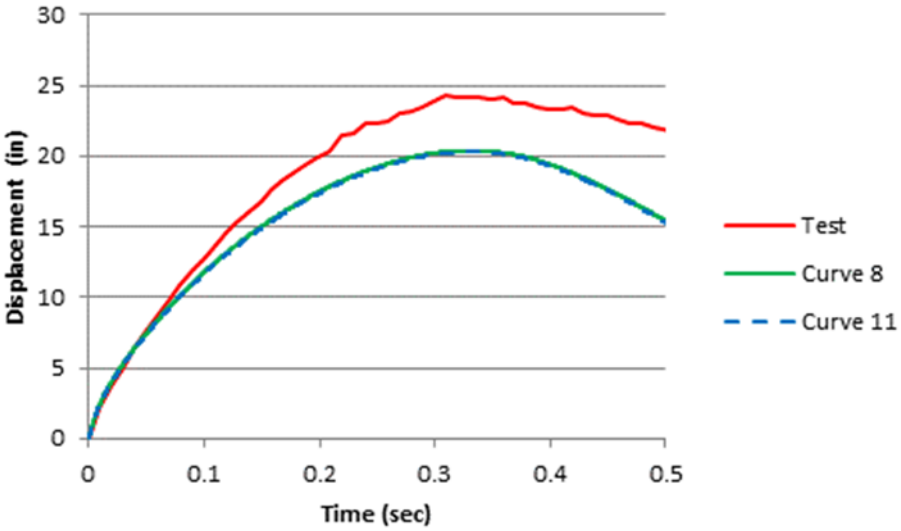


*Figure 18. Coupling Stiffness Plunge Depth Comparison*

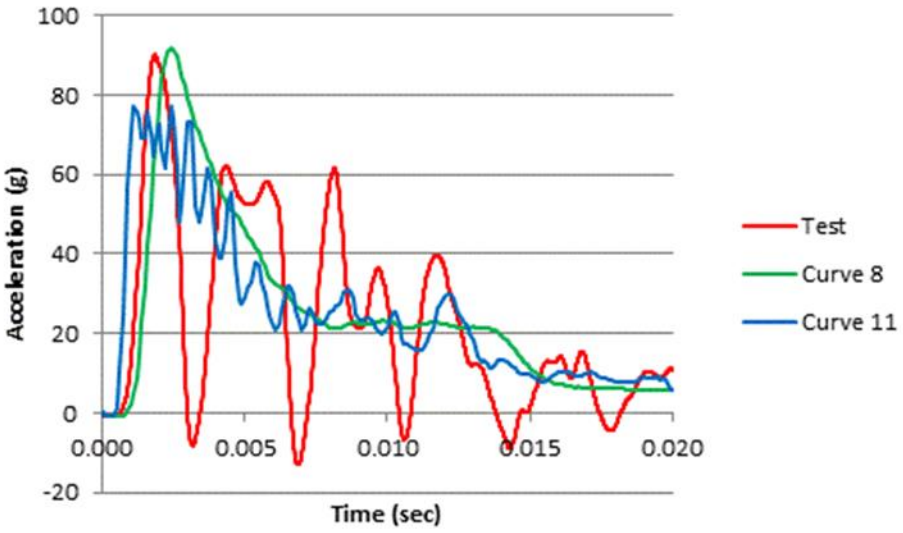


*Figure 19. Coupling Stiffness Acceleration Comparison*

The pressure distributions acting on the simulation model variants at 0.002 seconds are illustrated in Figure 20. No pressure data was recorded during the plunge depth test series, but it is known from previous works that the pressure distribution from the water impact should exhibit the "Coliseum Effect" [4] in which a narrow band of high pressure exists at the perimeter of the contact patch with much lower pressure toward the middle. The Curve 11 pressure distribution exhibits a stronger coliseum effect, but the secondary bands that exist toward the middle of the contact patch suggest significant oscillation in the pressure history. In the absence of test data, it is difficult to say which pressure distribution is more accurate. If the coupling stiffness is too soft, the pressure distribution appears more uniform or possibly shows a peak near the center of the contact patch. If the coupling stiffness is too high, the pressure distribution appears as a series of isolated spikes. Both of the pressure distributions shown in the figure should be considered to be in the plausible range.

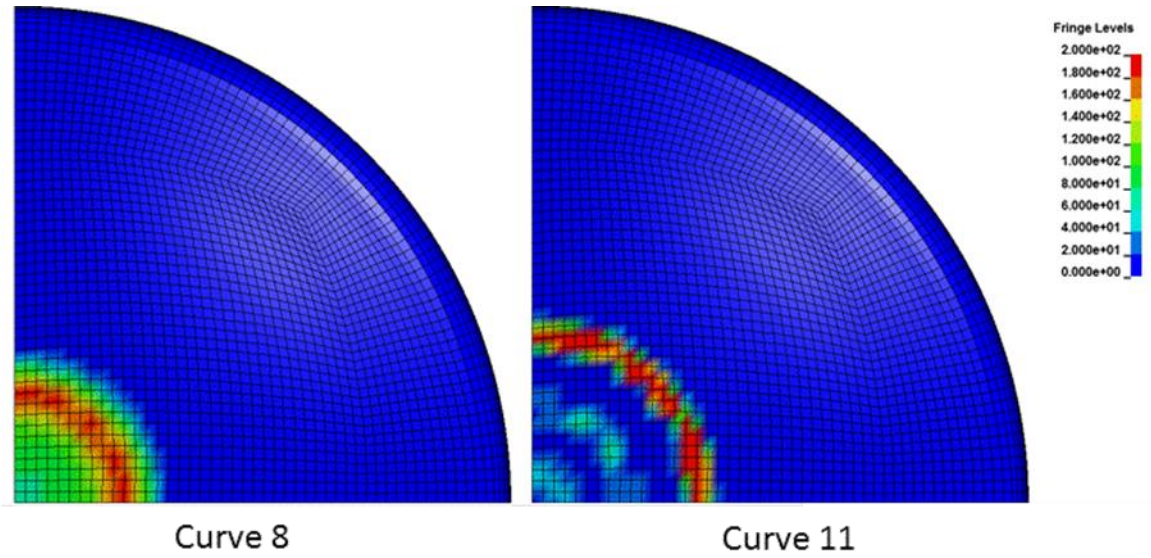


*Figure 20. Pressure Distributions for Coupling Stiffness Variants at 0.002 seconds*

## 7. Conclusions

The following are the principal conclusions for the plunge depth study.

1. LS-DYNA provides accurate predictions for peak accelerations.
2. LS-DYNA consistently under-predicts plunge depth. An allowance of at least 20% should be added to the LS-DYNA predictions.
3. The LS-DYNA predictions for plunge depth are relatively insensitive to the fluid-structure coupling stiffness.

## References


[1] Hallquist, J.O., "LS-DYNA Theoretical Manual", LSTC Livermore, 1998.

[2] Vassilakos, Gregory J., "Simulation of Elemental Water Impact Tests of a 20-inch Penetrometer," LRC-SPL-PL-068, November 10, 2010.

[3] Vassilakos, Gregory J., "Simulation of Elemental Water Impact Tests of a 36-inch Aluminum Tank Head," LRC-SPL-PL-069, Date TBD.

[4] "Final Test Report, Water Impact Test 74, Boilerplate 28 (Drop 1)", SID 66-33, North American Aviation, Inc., 15 March 1967.

## Appendix A: LS-DYNA Model

The following are the LS-DYNA cards that control the water properties, initial conditions, and fluid-structure coupling. These particular cards are for the Curve 8 coupling stiffness.

```
*KEYWORD
*SET_PART_LIST
      5500
       501       502       511       512
*SET_PART_LIST
      5501
       501       511
*SET_PART_LIST
      5502
       502       512
*ALE_MULTI-MATERIAL_GROUP
$       sid    idtype
      5501         0
      5502         0
*SET_MULTI-MATERAIL_GROUP_LIST
       123
         2
*CONTROL_ALE
$#     dct      nadv      meth      afac      bfac      cfac      dfac      efac
         2         1         2      -1.0
$#   start       end     aafac     vfact      prit       ebc      pref   nsidebc
                                                                 14.7
$
*SET_PART_LIST
$     psid
       502
        11
*CONSTRAINED_LAGRANGE_IN_SOLID
$    slave    master     sstyp     mstyp     nquad     ctype     direc     mcoup
       502      5500         0         0         1         4         2      -123
$    start       end      pfac      fric    frcmin      norm   normtyp      damp
         0         0        -8                 0.5                 1       0.5
$       cq      hmin      hmax     ileak     pleak   lcidpor     nvent    iblock

$   iboxid   ipenchk   intforc   ialesof    lagmul    pfacmm      thkf
                            1
$
*DEFINE_CURVE
$     lcid      sidr       sfa       sfo
         8                 1.0     1.000
                0.00                 0.0
               0.025               1.167
               0.050               2.964
               0.075               5.732
               0.100               9.994
               0.125              16.558
               0.150              26.666
               0.175              42.233
               0.200              66.205
               0.225             103.123
$
*SECTION_SOLID
$       SID    ELFORM       AET
       501        11
*SECTION_SOLID
$       SID    ELFORM       AET
       502        11
*SECTION_SOLID
$       SID    ELFORM       AET
       511        11         4
*SECTION_SOLID
$       SID    ELFORM       AET
```

```
       512        11         4
$
*PART
Air
$      PID     SECID       MID     EOSID      HGID      GRAV     ADAPT      TMID
       501       501       501       501       501         0
$
*PART
Water
$      PID     SECID       MID     EOSID      HGID      GRAV     ADAPT      TMID
       502       502       502       502       502         0
$
*PART
Air Reservoir
$      PID     SECID       MID     EOSID      HGID      GRAV     ADAPT      TMID
       511       511       501       501       501         0
$
*PART
Water Reservoir
$      PID     SECID       MID     EOSID      HGID      GRAV     ADAPT      TMID
       512       512       502       502       502         0
$
$
*MAT_NULL
$      mid       rho        pc        mu     terod     cerod        ym        pr
       501  1.127E-7     -0.01
*MAT_NULL
$      mid       rho        pc        mu     terod     cerod        ym        pr
       502 9.3365e-5     -0.01 1.6300E-7 0.0000000 0.0000000
$
*EOS_LINEAR_POLYNOMIAL
$    eosid        c0        c1        c2        c3        c4        c5        c6
       501       0.0       0.0       0.0       0.0       0.4       0.4       0.0
$       e0        v0
     36.74       0.0
$
*EOS_LINEAR_POLYNOMIAL
$    eosid        c0        c1        c2        c3        c4        c5        c6
       502      14.7 3.11574e5 0.0000000 0.0000000 0.0000000 0.0000000
$       e0        v0
       0.0       0.0
$
*Hourglass
$     HGID       IHQ        QM
       501         1     1.E-6
       502         1     1.E-6
*LOAD_BODY_X
         1    -386.1
*DEFINE_CURVE
         1         0       1.0       1.0       0.0       0.0         0
                 0.0                 1.0
               100.0                 1.0
*SET_PART_LIST
$      sid
      5781
$     pid1      pid2
       501       502
*INITIAL_HYDROSTATIC_ALE
$      SID   SIDTYPE     VECID   GRAVITY     PBASE
      5781         0      5789     386.1      14.7
$      NID  MMGBELOW
   8179400         1
   8000017         2
*SET_PART_LIST
$      sid
      5782
$     pid1      pid2
       511       512
*ALE_AMBIENT_HYDROSTATIC
$      SID   SIDTYPE     VECID   GRAVITY     PBASE
```

```
      5782         0      5789     386.1      14.7
$       NID  MMGBELOW
   8179400         1
   8000017         2
*DEFINE_VECTOR
$       vid        xt        yt        zt        xh        yh        zh       cid
      5789        0.        0.        0.        1.        0.        0.
$
*BOUNDARY_SPC_SET
         1         0         1         0         0         0         0         0
         2         0         1         0         0         0         0         0
         3         0         0         1         0         0         0         0
         4         0         0         0         1         0         0         0
         5         0         0         1         1         0         0         0
*END
```

# REPORT DOCUMENTATION PAGE

*Form Approved*
*OMB No. 0704-0188*



| 1. REPORT DATE *(DD-MM-YYYY)* | 2. REPORT TYPE | 3. DATES COVERED *(From - To)* |
|---|---|---|
| 01- 12 - 2014 | Contractor Report | October 2013 - September 2014 |

**4. TITLE AND SUBTITLE**

Elemental Water Impact Test: Phase 3 Plunge Depth of a 36-inch Aluminum Tank Head

**5a. CONTRACT NUMBER**

NNL12AA09C

**5b. GRANT NUMBER**

**5c. PROGRAM ELEMENT NUMBER**

**6. AUTHOR(S)**

Vassilakos, Gregory J.

**5d. PROJECT NUMBER**

**5e. TASK NUMBER**

**5f. WORK UNIT NUMBER**

747797.06.13.06.32.04.03

**7. PERFORMING ORGANIZATION NAME(S) AND ADDRESS(ES)**

NASA Langley Research Center
Hampton, Virginia 23681

**8. PERFORMING ORGANIZATION REPORT NUMBER**

**9. SPONSORING/MONITORING AGENCY NAME(S) AND ADDRESS(ES)**

National Aeronautics and Space Administration
Washington, DC 20546-0001

**10. SPONSOR/MONITOR'S ACRONYM(S)**

NASA

**11. SPONSOR/MONITOR'S REPORT NUMBER(S)**

NASA/CR-2014-218666

**12. DISTRIBUTION/AVAILABILITY STATEMENT**

Unclassified - Unlimited
Subject Category 31
Availability: NASA STI Program (757) 864-9658

**13. SUPPLEMENTARY NOTES**

Langley Technical Monitor: Robin C. Hardy

**14. ABSTRACT**

Spacecraft are being designed based on LS-DYNA water landing simulations. The Elemental Water Impact Test (EWIT) series was undertaken to assess the accuracy of LS-DYNA water impact simulations. Phase 3 featured a composite tank head that was tested at a range of heights to verify the ability to predict structural failure of composites. To support planning for Phase 3, a test series was conducted with an aluminum tank head dropped from heights of 2,6,10, and 12 feet to verify that the test article would not impact the bottom of the test pool. This report focuses on the comparisons of the measured plunge depths to LS-DYNA predictions.

**15. SUBJECT TERMS**

Accelerations; Composite; Fluid-structure coupling; LS-DYNA; Plunge; Simulations; Water

| 16. SECURITY CLASSIFICATION OF: | | | 17. LIMITATION OF ABSTRACT | 18. NUMBER OF PAGES | 19a. NAME OF RESPONSIBLE PERSON |
|---|---|---|---|---|---|
| a. REPORT | b. ABSTRACT | c. THIS PAGE | | | STI Help Desk (email: help@sti.nasa.gov) |
| | | | | | 19b. TELEPHONE NUMBER *(Include area code)* |
| U | U | U | UU | 28 | (757) 864-9658 |